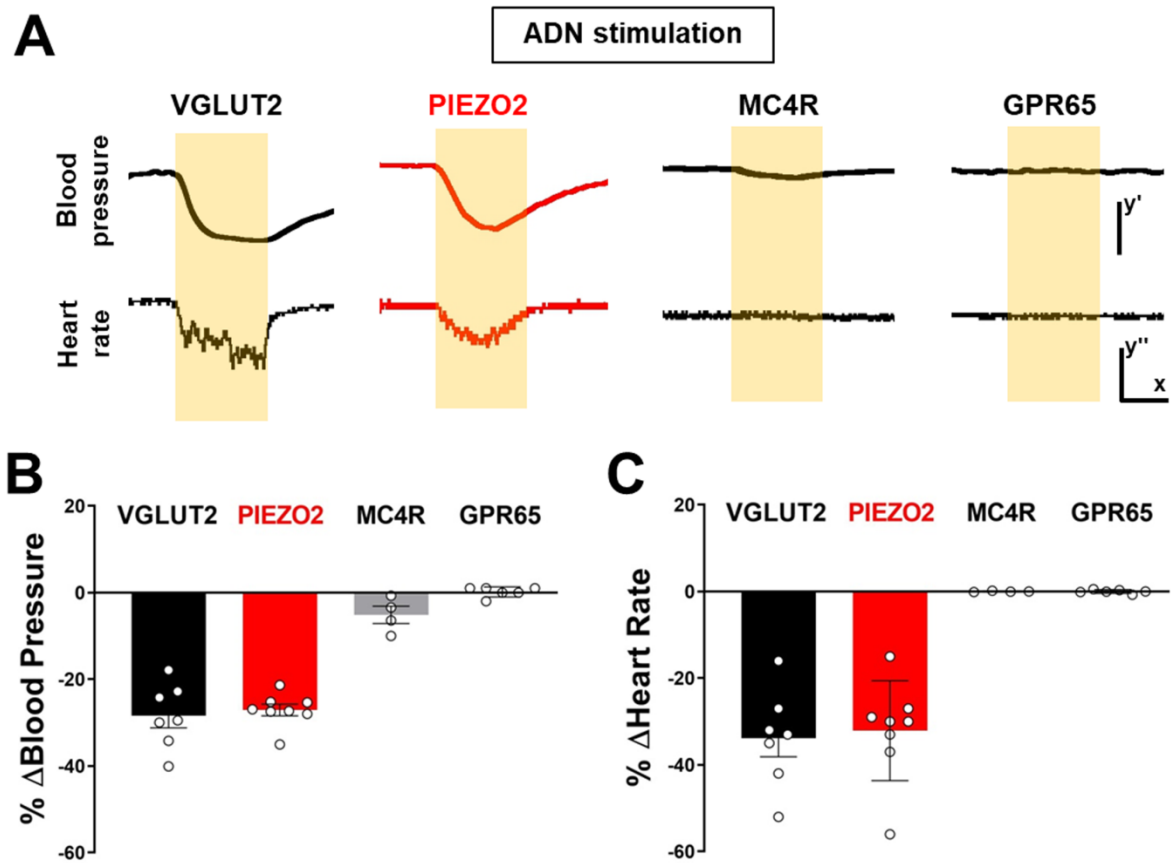


**Cell Reports, Volume 29**

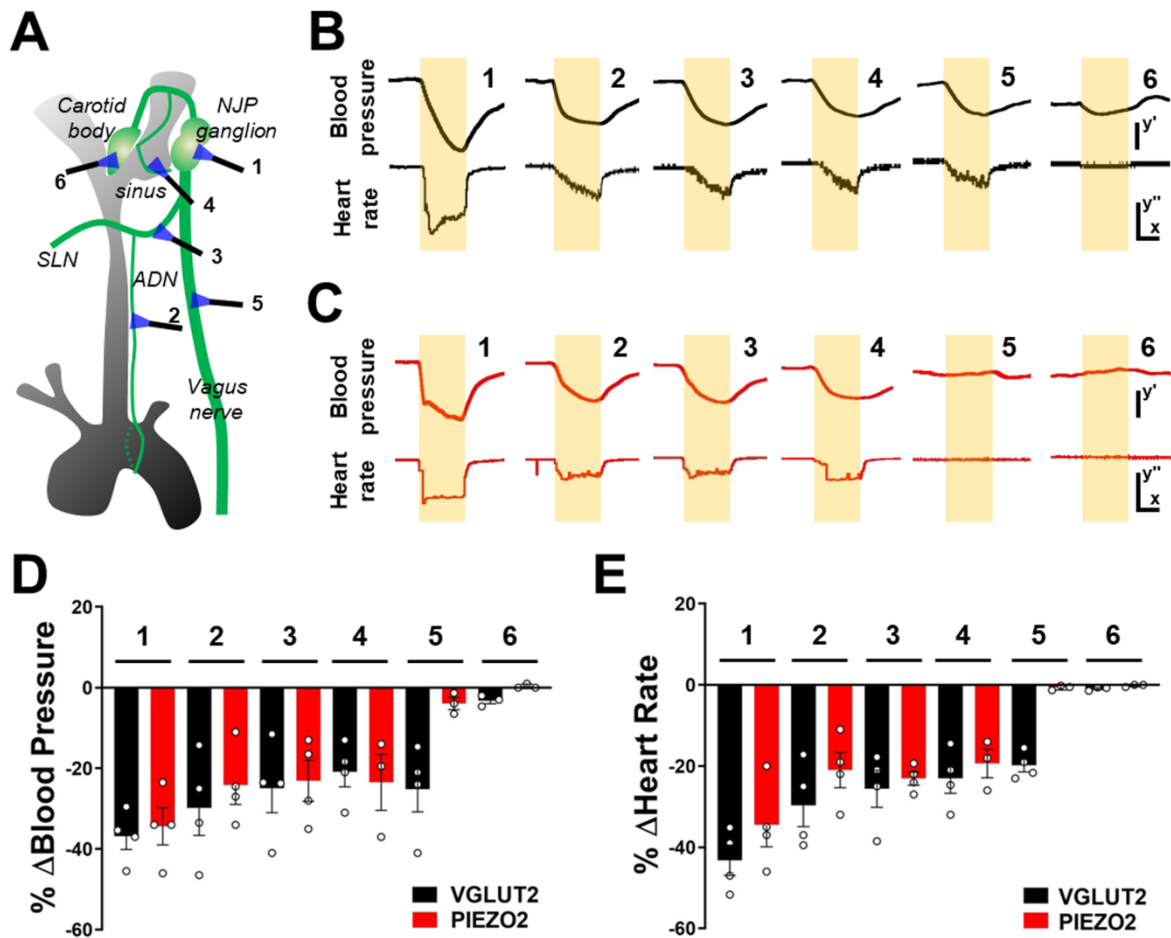
**Supplemental Information**

**Arterial Baroreceptors Sense Blood Pressure  
through Decorated Aortic Claws**

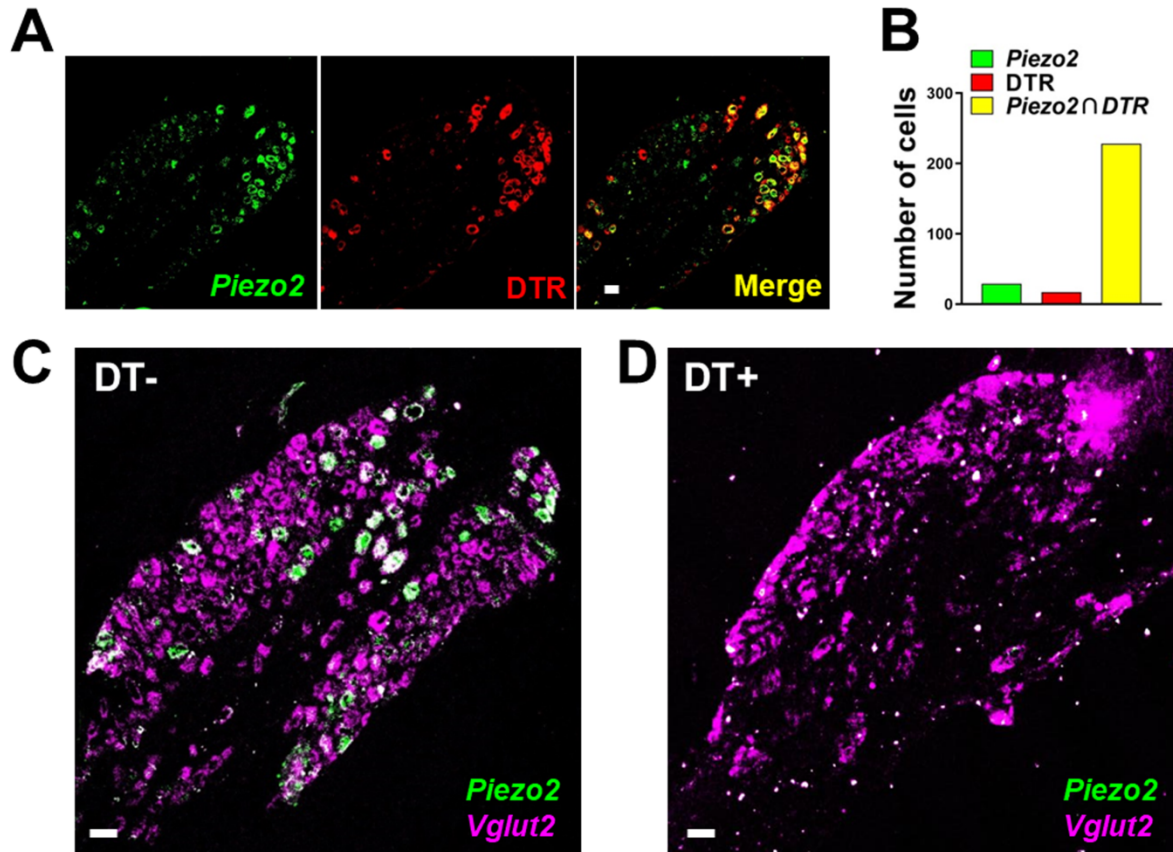
**SooHong Min, Rui B. Chang, Sara L. Prescott, Brennan Beeler, Narendra R. Joshi, David E. Strohlic, and Stephen D. Liberles**



**Figure S1. Optogenetic activation of sensory neurons in the aortic depressor nerve (Related to Figure 1).** (A) Representative traces of blood pressure and heart rate with optogenetic stimulation (yellow shading) of the aortic depressor nerve in VGLUT2 (*Vglut2-ires-Cre; loxP-ChR2*), PIEZO2 (*Piezo2-ires-Cre; loxP-ChR2*, red), MC4R (*Mc4r-2a-Cre; loxP-ChR2*), and GPR65 (*Gpr65-ires-Cre; loxP-ChR2*) mice, scale bars: y': 20 mmHg, x: 5 sec, y'': 100 BPM. Quantifying changes in blood pressure (B) and heart rate (C) following illumination of the aortic depressor nerve in mice indicated, n: 4-8, mean  $\pm$  sem.



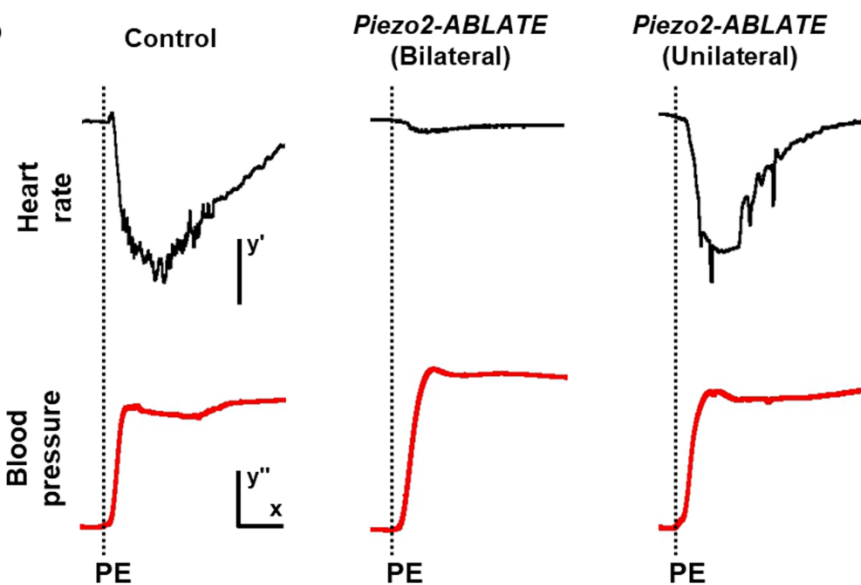
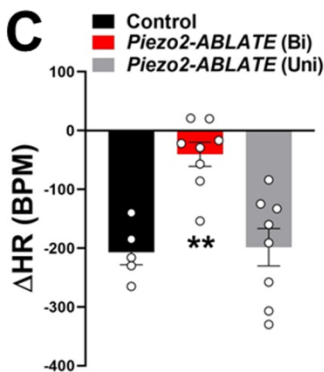
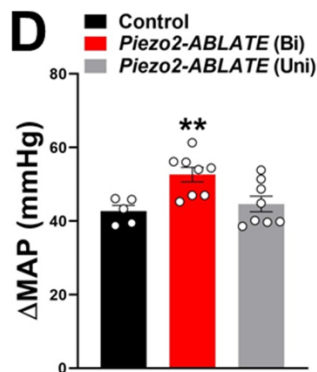
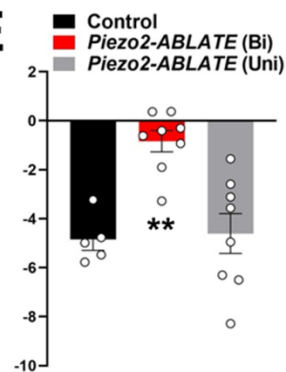
**Figure S2. Nerve branch-selective optogenetics (Related to Figure 1).** (A) Cartoon depicting various sites of optogenetic stimulation, including 1: NJP ganglion, 2: aortic depressor nerve (ADN), 3: superior laryngeal nerve (SLN), 4: carotid sinus, 5: vagal trunk after departure of SLN, and 6: carotid body. Representative traces of blood pressure and heart rate with optogenetic stimulation (yellow shading) occurring at sites indicated (1-6 from panel A) in *Vglut2-ires-Cre; loxP-ChR2* (B, black) and *Piezo2-ires-Cre; loxP-ChR2* (C, red) mice, scale bars: y': 20 mmHg, x: 5 sec, y'': 100 BPM. Quantifying changes in blood pressure (D) and heart rate (E) following optogenetic stimulation of *Vglut2-ires-Cre; loxP-ChR2* (black) and *Piezo2-ires-Cre; loxP-ChR2* (red) mice, n: 3-4, mean  $\pm$  sem).



**Figure S3. Assessing specificity of PIEZO2 neuron targeting in *Piezo2-ABLATE* mice (Related to Figure 2).** (A) Sequential *in situ* hybridization for *Piezo2* transcript (green) and immunocytochemistry for DTR (red) in cryosections of vagal ganglia from *Piezo2-ires-Cre; loxP-DTR* mice, scale bar: 20  $\mu$ m. (B) Counts of cells expressing only *Piezo2* (green), only DTR (red), or both (yellow), n: 5 sections from 2 mice. Two color *in situ* hybridization using cRNA probes that recognize *Piezo2* (green) and *Vglut2* (magenta) in cryosections of vagal ganglia from *Piezo2-ires-Cre; loxP-DTR* mice treated (C) without or (D) with DT, scale bar: 30  $\mu$ m.

**A**

Blood pressure (mmHg)	Control	<i>Piezo2</i> -ABLATE (Bilateral)	<i>Piezo2</i> -ABLATE (Unilateral)
Mean	66.33	69.92	69.43
Standard Error	±4.775	±2.237	±4.657

**B****C****D****E**

**Figure S4. Loss of baroreceptor reflex requires bilateral ablation of PIEZO2 neurons in NJP ganglia (Related to Figure 2).** (A) Resting blood pressure of *loxP-DTR* mice injected bilaterally with DT (control) and *Piezo2-ires-Cre; loxP-DTR* mice injected unilaterally or bilaterally with DT. (B) Assessment of baroreflex integrity in *loxP-DTR* mice injected bilaterally with DT (control), and *Piezo2-ires-Cre; loxP-DTR* mice injected unilaterally or bilaterally with DT. Representative effects of phenylephrine injection (dashed line) on blood pressure and heart rate, scale bars, y': 100 BPM, x: 10 sec, y'': 20 mmHg. Quantification of phenylephrine (PE)-induced change in heart rate or HR (C), change in mean arterial blood pressure or MAP (D), and baroreflex (E), defined as change in HR ( $\Delta$  BPM) divided by change in BP ( $\Delta$  mmHg), n: 5-8, mean  $\pm$  sem, \*\*p<.005.

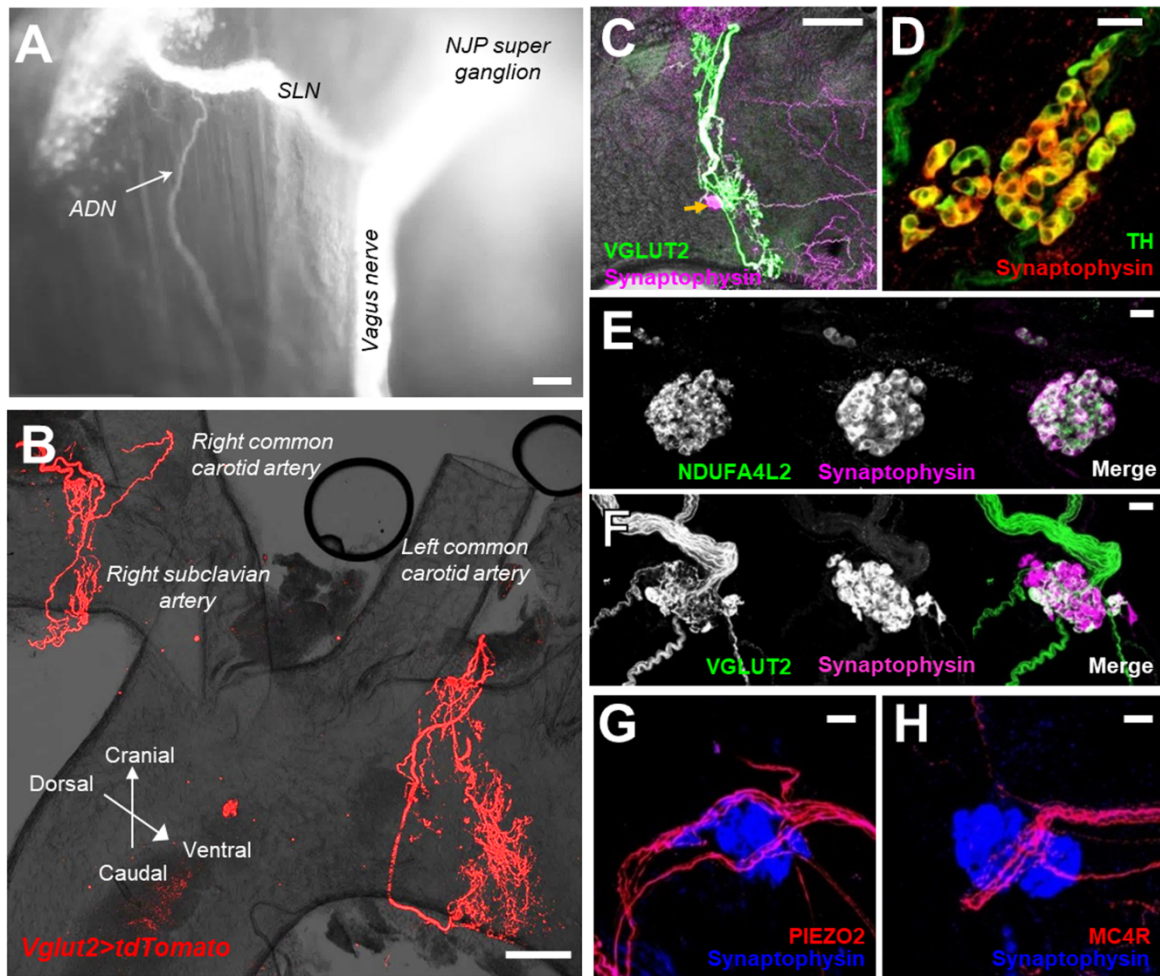


**Figure S5. Visualizing innervation of the carotid sinus (Related to Figure 5).** (A) Wholemount image of native fluorescence from the aortic depressor nerve (ADN) and superior laryngeal nerve (SLN) after ganglion injection of *AAV-Gfp* in wild type mice, scale bar 100  $\mu\text{m}$ . (B) Wholemount anti-tdTomato immunofluorescence of the great aortic vessels in *Vglut2-ires-Cre; loxP-tdTomato* mice, scale bar 300  $\mu\text{m}$ . (C) Aortic arch immunohistochemistry for tdTomato (green) and synaptophysin (magenta) after injection of *AAV-flex-tdTomato* into NJP ganglia of *Vglut2-ires-Cre* mice, yellow arrow indicates location of an aortic body, scale bar 300  $\mu\text{m}$ . (D) Aortic arch immunohistochemistry for tyrosine hydroxylase (green) and synaptophysin (red), scale bar 20  $\mu\text{m}$ . (E) Aortic body immunohistochemistry for NDUFA4L2 (green) and synaptophysin (magenta), scale bar 20  $\mu\text{m}$ . (F) Aortic body immunohistochemistry for tdTomato (green) and synaptophysin (magenta) after injection of *AAV-flex-tdTomato* into NJP ganglia of *Vglut2-ires-Cre* mice, scale bar 20  $\mu\text{m}$ . Two color immunohistochemistry for synaptophysin (blue) and tdTomato (red) to visualize neuronal fibers of passage labeled by injection of *AAV-flex-tdTomato* into NJP ganglia of *Piezo2-ires-Cre* mice (G) and *Mc4r-2a-Cre* mice (H), scale bar 20  $\mu\text{m}$ .

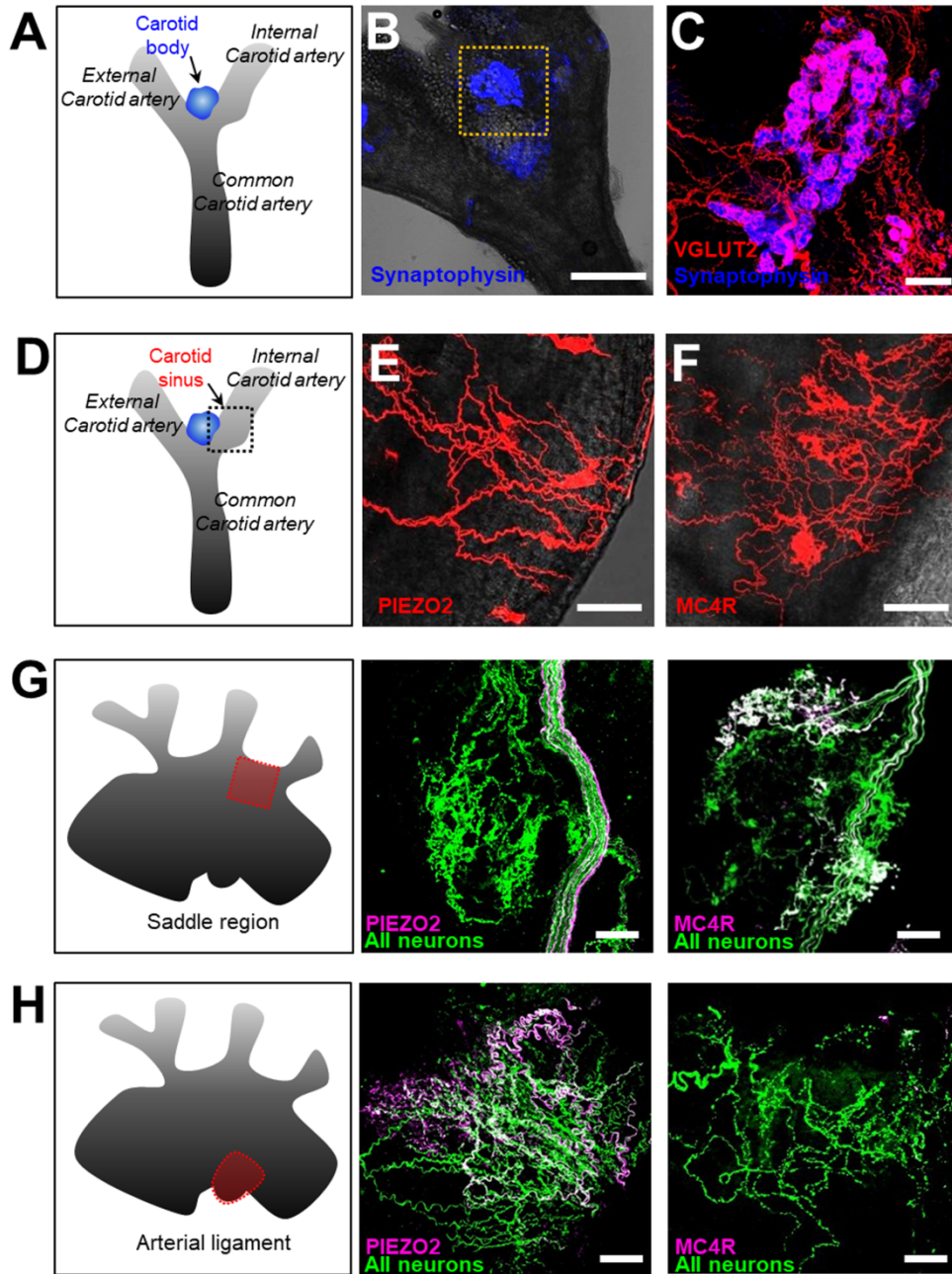


**Figure S6. Neuron subtypes that innervate the carotid sinus and aortic arch (Related to Figure 5).** (A, D) Cartoon depictions of the carotid sinus. Carotid glomus cells can be visualized (blue) by immunostaining for synaptophysin (B-C). Vagal afferents were visualized by immunocytochemistry for tdTomato (red) following injection of *AAV-flex-tdTomato* into NJP ganglia of *Vglut2-ires-Cre* mice (C), *Piezo2-ires-Cre* mice (E), and *Mc4r-2a-Cre* mice (F), scale bars: 400  $\mu\text{m}$  for B; 20  $\mu\text{m}$  for C; 100  $\mu\text{m}$  for E-F. Boxed region in B depicts regions of analysis for panels C, while boxed region in D depicts region of analysis for E-F. Representative images used for quantitative analysis of flower spray terminals in the aortic saddle region (G) and end-net endings in the arterial ligament (H). Vagal afferents were visualized by immunocytochemistry following injection of Cre-independent *AAV-Gfp* (green, ALL NEURONS) and *AAV-flex-tdTomato* (magenta) into NJP ganglia of *Piezo2-ires-Cre* (PIEZO2) or *Mc4r-2a-Cre* (MC4R) mice, scale bar 30  $\mu\text{m}$ .

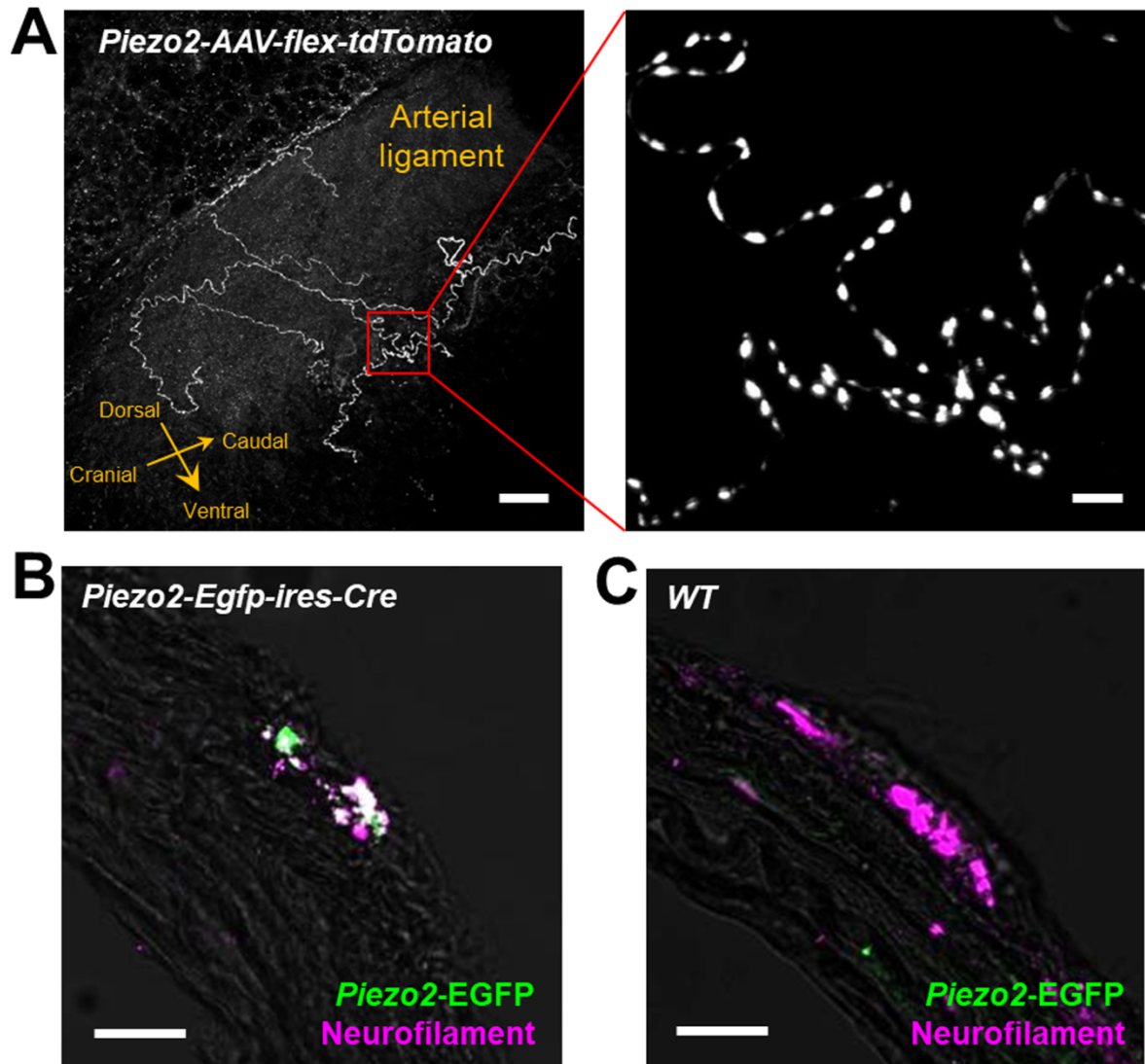


**Figure S7. Sensory neuron innervation of the arterial ligament (Related to Figure 7).** (A) Vagal afferents were visualized in the arterial ligament by immunohistochemistry for tdTomato following injection of *AAV-flex-tdTomato* into NJP ganglia of *Piezo2-ires-Cre* mice, scale bars, left: 30  $\mu\text{m}$ , right: 10  $\mu\text{m}$ . The right panel is a high magnification, partial Z-stack image from a region (red box) of the left image. Immunohistochemistry for GFP (green) and neurofilament (magenta) in arterial ligament of (B) *Piezo2-ires Cre* and (C) wild type mice. *Piezo2-ires-Cre* mice express a PIEZO2-GFP fusion protein from the endogenous *Piezo2* locus, scale bars: 10  $\mu\text{m}$ .